

## Comparison of the Electrochemical and Enzymic Oxidation of 1,3,7-Trimethyluric Acid at Solid Electrodes

Rajendra Nath Goyal,\* Ajay Kumar Jain, and Neena Jain

Department of Chemistry, University of Roorkee, Roorkee-247667, India

(Received October 4, 1995)

The electrochemical oxidation of 1,3,7-trimethyluric acid has been studied in phosphate buffers in the pH range 2.1–10.2 at solid electrodes. In cyclic voltammetry a single, well defined, pH-dependent oxidation peak was obtained at all of the three electrodes used. However, the reduction behavior of the oxidation product was different at pyrolytic graphite, glassy carbon (GCE), and platinum due to adsorption at PGE and GCE. The nature of the electrode reaction was established as EC, in which a charge transfer is followed by competitive chemical reactions. The formation of the same UV-absorbing intermediate and products and identical rate constants for the decay of the UV-absorbing intermediate indicated that the electrochemical oxidation of 1,3,7-trimethyluric acid proceeds by an identical mechanism at PGE, GCE, and Pt. The results of a peroxidase-catalyzed oxidation of 1,3,7-trimethyluric acid were compared with the electrochemical oxidation; it is concluded that both of the oxidations follow a similar pathway.

Spectral studies during the electrochemical oxidation of naturally occurring heterocyclic molecules have been found to provide uniquely invaluable insights into the biological behavior of such molecules.<sup>1)</sup> For a number of years now this laboratory has been investigating the electrochemical and peroxidase catalyzed oxidation of various naturally occurring purines in the expectation that the redox mechanism of such molecules will provide useful information concerning their metabolic behavior.<sup>2–4)</sup> It has also been found in these investigations that spectral studies during oxidation provide information about the UV-visible absorbing intermediate and that the presence of an electron-releasing methyl group in purines affects the ease of oxidation, while also altering the mechanism by restricting the number of resonating structures. Besides this, it has also been observed that the electrochemical and enzymic oxidation of these compounds proceed by an identical EC mechanism, and that the same intermediates and products are formed in both types of oxidations. This paper presents the results obtained from spectral studies coupled with the electrochemical oxidation of 1,3,7-trimethyluric acid (compound I) at solid electrodes. A comparison of the electrochemical oxidation with peroxidase-catalyzed oxidation is also presented.

### Experimental

1,3,7-Trimethyluric acid was obtained from Adams Chemical Company, Round Lake, IL, USA, and was used as received. Experiments were carried out in phosphate buffers<sup>5)</sup> having an ionic strength of 0.25 M (1 M = 1 mol dm<sup>-3</sup>); all of the potentials were referred to the SCE at an ambient temperature of 20 ± 2 °C. Type-VIII peroxidase ( $R_z \approx 3.4$ ), isolated from horseradish peroxidase for enzymic oxidation, was obtained from Sigma Chemical Co. Hydrogen peroxide was obtained from BDH and catalase was a product of the CSIR Centre for biochemicals, New Delhi.

Linear and cyclic sweep voltammetric studies were carried out

using a micronics cyclic voltammeter attached to a omniscrite  $x-y-t$  recorder. The methods used for fabricating pyrolytic graphite (PGE), platinum (Pt), and glassy carbon electrodes (GCE) were essentially the same as those described earlier.<sup>6)</sup>

The surface area of PGE, GCE, and Pt used as a working electrode were ca. 90 mm<sup>2</sup>, ca. 12 mm<sup>2</sup>, and ca. 3 mm<sup>2</sup>, respectively. Renewal of the platinum and PGE surface after each voltammogram was carried out by polishing on a 600 grit metallographic polishing disc, whereas that of GCE was done by a method suggested by Chan et al.<sup>7)</sup> The coulometric experiments were carried out using a conventional three-compartment cell. A pyrolytic graphite plate (6 × 1 cm<sup>2</sup>) or platinum foil (2 × 2 cm<sup>2</sup>) or a glassy carbon rod (6 cm length, 0.25 cm radius) was used as a working electrode, platinum gauze as a counter electrode and SCE as a reference electrode. The number of electrons ( $n$ ) was determined by a graphical integration of the current–time curve, as reported in the literature by Lingane.<sup>8)</sup> The spectral changes during oxidation and the kinetics of the UV-absorbing intermediate were monitored in a 1.0 cm quartz cell using a Beckmann DU-6 spectrophotometer. The mass spectra were recorded using a JEOL JMS D 300 instrument, and the <sup>1</sup>H NMR were recorded using a Varian XL 300 spectrometer in [<sup>2</sup>H<sub>6</sub>] DMSO-*d*<sub>6</sub>.

**Procedure.** Voltammetric studies were carried out by mixing 2.0 ml of the stock solution of compound I (1 mM) prepared in doubly distilled water with 2.0 ml of a phosphate buffer ( $\mu = 0.5$  M) of appropriate pH. The solution was deaerated by passing a stream of nitrogen gas for 12–15 min before recording the voltammograms.

The enzymic oxidation of 1,3,7-trimethyluric acid was carried out by mixing 2 ml of compound I (0.1 mM) and 0.5 ml (0.002 mM) of horseradish peroxidase (mol wt 20000) and 0.5 ml of hydrogen peroxide (0.6 mM) prepared in a phosphate buffer of the same pH and having an ionic strength of 0.25 mM. The reaction was terminated by adding a 1 ml catalase solution (1 mg ml<sup>-1</sup>) prepared in a buffer of the same pH. Products of the electrooxidation of 1, 3,7-trimethyluric acid were characterized at pH 3.0 and 7.0. For this purpose 8–10 mg of 1,3,7-trimethyluric acid was exhaustively electrolyzed at a potential 100 mV more positive than the peak po-

tential. The progress of the electrolysis was monitored by recording cyclic voltammograms at different time intervals. When the oxidation peak completely disappeared the electrolyzed solution was removed from the cell and lyophilized. The obtained freeze-dried material was dissolved in water and passed through a glass column packed with Sephadex G-10 (bead size 40–120  $\mu\text{m}$ ) using double-distilled water as the eluting solvent. Fractions of 5.0 ml each were collected, and the absorbance of each fraction was measured at 210 nm using a Beckmann DU-6 spectrophotometer. The first peak at between 140–180 ml was found to give a positive test for phosphate with ammonium molybdate, and was thus discarded. The volumes under the other peaks were collected and lyophilized separately, and then analyzed by TLC, mp, IR, NMR, and mass spectra.

### Results and Discussion

The linear-sweep voltammetry of 1,3,7-trimethyluric acid in the pH range 2.1–10.2 and at a sweep rate of  $50 \text{ mV s}^{-1}$  exhibited one well-defined oxidation peak ( $I_a$ ) at all of the three electrodes used. The oxidation peak ( $I_a$ ) at PGE was found to be sharper compared to that of GCE and platinum. The peak at platinum was broader than that at GCE. The peak potential of peak  $I_a$  was dependent on the pH, and shifted towards a less positive potential along with an increase in the pH in the 2.0–6.0 range; at  $\text{pH} > 6.0$ , the peak potential was practically independent of the pH. The peak potential of peak  $I_a$  at PGE and GCE were more or less the same over the entire pH range; however, the values of  $E_p$  at platinum were approximately 20–30 mV less positive over the entire pH range studied. An  $E_p$ -versus-pH plot (Fig. 1) exhibited a break at around pH 6.0 at all three electrodes. This break corresponds to a  $pK_a$  value of 1,3,7-trimethyluric acid, and is similar to  $pK_a$  reported in the literature.<sup>9,10</sup> The dependence

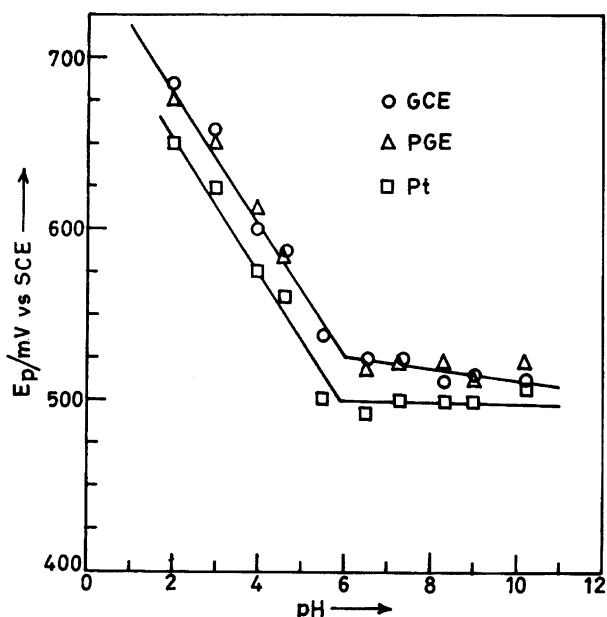


Fig. 1.  $E_p$  versus pH plot obtained for peak  $I_a$  for 0.5 mM 1,3,7-trimethyluric acid at different solid electrodes (sweep rate =  $50 \text{ mV s}^{-1}$ ).

of  $E_p$  on pH can be expressed by the following relations:

$$E_p(\text{pH } 2.1\text{--}6.0) = [750 - 35 \text{ pH}] \text{ mV vs. SCE at PGE/GCE}$$

and

$$E_p(\text{pH } 2.1\text{--}6.0) = [735 - 45 \text{ pH}] \text{ mV vs. SCE at platinum.}$$

The dependence of  $E_p$  on pH indicated that the electroactive species oxidized in a two-electron step is not the species which predominates in the bulk of the solution, but its conjugate base bearing one less proton is oxidized over the entire pH range used. As at  $\text{pH} > 6.0$ , since no protons are involved in oxidation, the peak potential is independent of the pH.

In cyclic voltammetry at a sweep rate of  $50 \text{ mV s}^{-1}$  a well-defined anodic peak ( $I_a$ ) was observed at all three electrodes, whereas in the reverse sweep a different behavior was observed. At PGE, three cathodic peaks ( $I_c$ ,  $II_c$ , and  $III_c$ ) were obtained, whereas at GCE and platinum only one cathodic peak ( $I_c$ ) was observed over the entire pH range. A comparison of the cyclic voltammograms of 1,3,7-trimethyluric acid at pH 7.3 at each of the three electrodes is presented in Fig. 2. Peak  $I_c$  formed a quasi-reversible couple with peak  $I_a$ , and the peak current of peak  $I_c$  increased along with an increase in the sweep rate. The ratio of peaks  $I_c/I_a$  also increased along with an increase in the sweep rate at all three electrodes, and reached 0.22 at PGE, 0.18 at platinum and 0.62 at GCE at  $1.0 \text{ V s}^{-1}$  (Table 1). It was thus concluded that the species

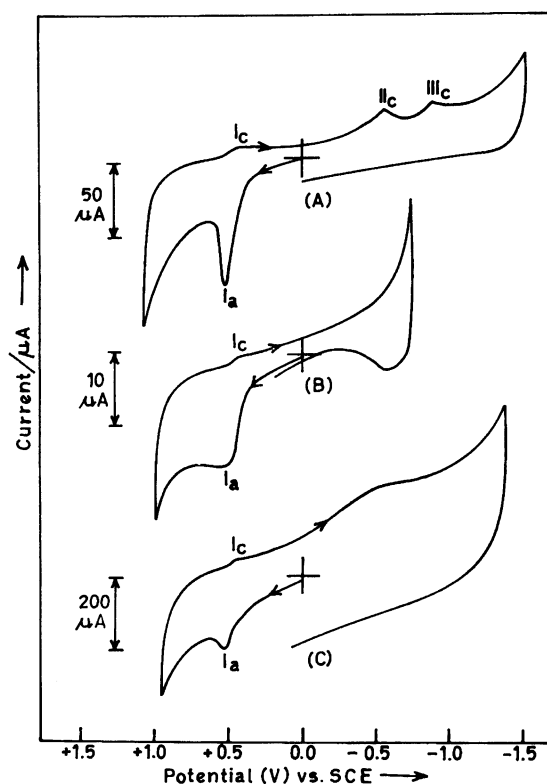


Fig. 2. Typical cyclic voltammograms of 0.5 mM 1,3,7-trimethyluric acid in phosphate buffers of pH 7.3 ( $\mu=0.25 \text{ M}$ ) at different solid electrodes (sweep rate =  $50 \text{ mV s}^{-1}$ ). (A) PGE, (B) Pt, (C) GCE.

Table 1. Ratio of Peaks  $I_c/I_a$  Observed at Different Sweep Rates for 0.5 mM 1,3,7-Trimethyluric Acid at Different Solid Electrodes at pH 7.3

Sweep rate/ $\text{mV s}^{-1}$	$I_c/I_a^{\text{a}}$		
	PGE	Pt	GCE
5	0.01	—	—
10	0.02	0.027	0.05
20	0.05	0.034	0.13
50	0.06	0.037	0.17
100	0.09	0.043	0.20
200	0.12	0.060	0.33
500	0.18	0.090	0.34
1000	0.22	0.180	0.62

a) Average of at least three replicate determinations.

responsible for peak  $I_c$  is unstable, and, hence, is more available in the vicinity of the electrode at higher sweep rates. Thus, it was concluded that the electrode reaction is coupled with consecutive chemical reactions. The peak current for peak  $II_c$  was also found to be dependent on the sweep rate. However, the ratio of peaks  $I_c/II_c$  remained practically constant (Table 2) at PGE. Peak  $II_c$  was not observed at the other electrodes used.

The effect of the concentration on peak  $I_a$  was also studied in the concentration range 0.1 mM to 1.0 mM at all three electrodes. The peak current of peak  $I_a$  increased along with an increase in the concentration at all three electrodes. The plot of  $i_p$  vs. the concentration was linear up to 0.4 mM at PGE (Fig. 3A) and up to 0.5 mM at GCE (Fig. 3B), and then became constant at higher concentrations, whereas at the platinum electrode the  $i_p$ -vs.-concentration graph was linear over the entire concentration range (Fig. 3C). This behavior indicated the adsorption of 1,3,7-trimethyluric acid at the surface of PGE and GCE. The adsorption of 1,3,7-trimethyluric acid was further confirmed by an increase in the peak current function along with an increase in  $\log v$  in the range 5  $\text{mV s}^{-1}$  to 1  $\text{V s}^{-1}$  at PGE and GCE<sup>11,12)</sup> (Fig. 4B). The values of  $i_p/\sqrt{v}$  did not change with an increase in the sweep rate at the platinum electrode surface, and, hence, indicated that the electrode reaction was free from adsorption complications at platinum.

At PGE, the ratio of peaks  $I_c/II_c$  was found to be 0.12, and was practically the same over the entire concentration range

Table 2. Observed Peak Current Values for 0.5 mM 1,3,7-Trimethyluric Acid for  $I_c/II_c$  at PGE at pH 7.3

Sweep rate/ $\text{mV s}^{-1}$	$I_c^{\text{a}}$	$II_c^{\text{a}}$	$I_c/II_c$
5	0.25	0.75	0.33
10	0.50	1.50	0.33
20	2.00	7.50	0.27
50	5.00	16.00	0.31
100	8.00	27.50	0.30
200	25.00	78.00	0.32
500	50.00	150.00	0.33
1000	90.00	258.00	0.35

a) Average of at least three replicate determinations.

used. The ratio of peaks  $II_c/III_c$  was also determined at PGE with an increase in the concentration of 1,3,7-trimethyluric acid, and was found to be 0.7. This ratio did not change even when the concentration of uric acid was changed from 0.1 to 1.0 mM.

The peak potential ( $E_p$ ) of peak  $I_a$  was also dependent on the sweep rate at all three electrodes used in the range 5  $\text{mV s}^{-1}$  to 1  $\text{V s}^{-1}$ . The peak potential was found to shift by 12–15 mV per ten-fold increase in the sweep rate in the range 5 to 100  $\text{mV s}^{-1}$ , whereas the shift decreased to 10 mV at higher sweep rates. The plot of  $\Delta E_{p/2}/\Delta \log v$  vs.  $\log v$  was S-shaped at all electrodes, suggesting that the nature of the electrode reaction is EC, in which charge transfer is followed by an irreversible chemical reaction.<sup>13)</sup>

A controlled potential electrolysis of 1,3,7-trimethyluric acid was carried out in phosphate buffers of different pH at PGE, GCE, and platinum electrodes by a graphical integration of the current–time curve. Although the nature of the  $i_p$ -versus-time plot was exponential at all of the electrodes, the plot of  $\log i_p$  versus time was a straight line for the first 20–25 min of electrolysis, after which a large deviation from a straight line was noticed. This behavior suggested that the electrode reaction followed a simple path for the first 20–25 min of electrolysis, and thereafter competitive chemical reactions played a significant role in the bulk cleavage of the product, as suggested by Meites<sup>14)</sup> and Cauquis et al.<sup>15)</sup> The average experimental  $n$  values obtained under different conditions are summarized in Table 3, and are close to  $2.0 \pm 0.3$ .

**Spectral Studies.** The UV spectra of 1,3,7-trimethyluric acid were recorded over the entire pH range 2.1–10.2 to determine the  $pK_a$  value. The solution of 1,3,7-trimethyluric acid (0.1 mM) exhibited three absorption bands at 288, 236, and 200 nm below pH 6.0, whereas at higher pH the band at 236 nm changed to a shoulder. The absorbance at  $\lambda_{\text{max}}$  was plotted against the pH; the resulting dissociation curve shows inflection at around pH 6.0 which corresponds to a

Table 3. Coulometric  $n$ -Value Observed for the Electrooxidation of 1,3,7-Trimethyluric Acid

pH	Concn mM	Electrode	Pot. (V) vs. SCE	Experimental $n$ -values <sup>a)</sup>
2.0	0.1	PGE	0.80	1.86
	0.1	GCE	0.80	1.92
	0.1	Pt	0.80	2.06
4.0	0.1	PGE	0.70	1.88
	0.2	GCE	0.70	1.92
	0.5	GCE	0.70	2.02
6.5	0.5	Pt	0.70	1.86
	0.5	GCE	0.60	1.90
	0.5	Pt	0.60	1.92
8.3	0.2	PGE	0.55	2.06
	0.5	GCE	0.55	1.88
	0.5	Pt	0.55	1.90
9.0	0.5	GCE	0.55	2.10
	0.5	Pt	0.55	1.90

a) Average of at least three replicate determinations.

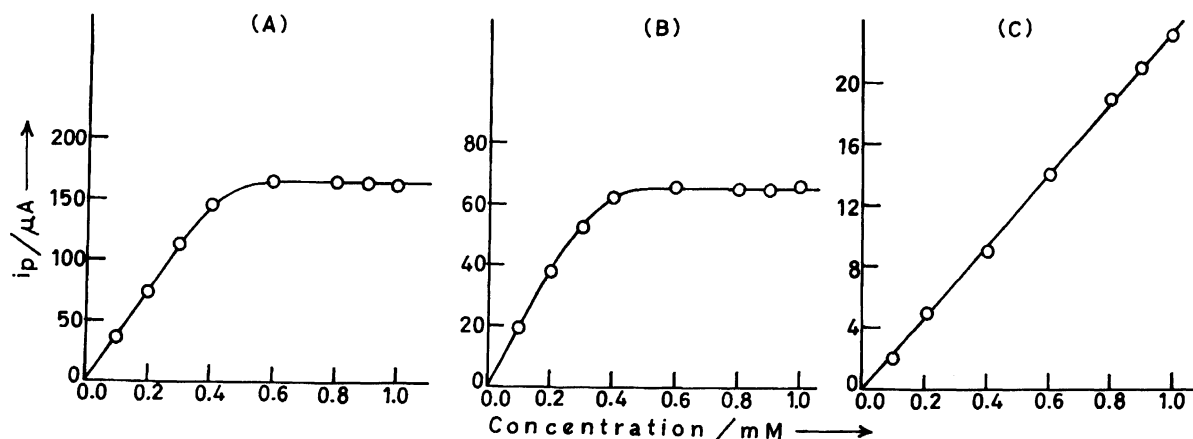


Fig. 3. Dependence of peak current for the oxidation peak  $I_a$  of 1,3,7-trimethyluric acid on concentration at different solid electrodes, pH=7.3, sweep rate=50 mV s<sup>-1</sup>. (A) PGE, (B) GCE, (C) Pt.

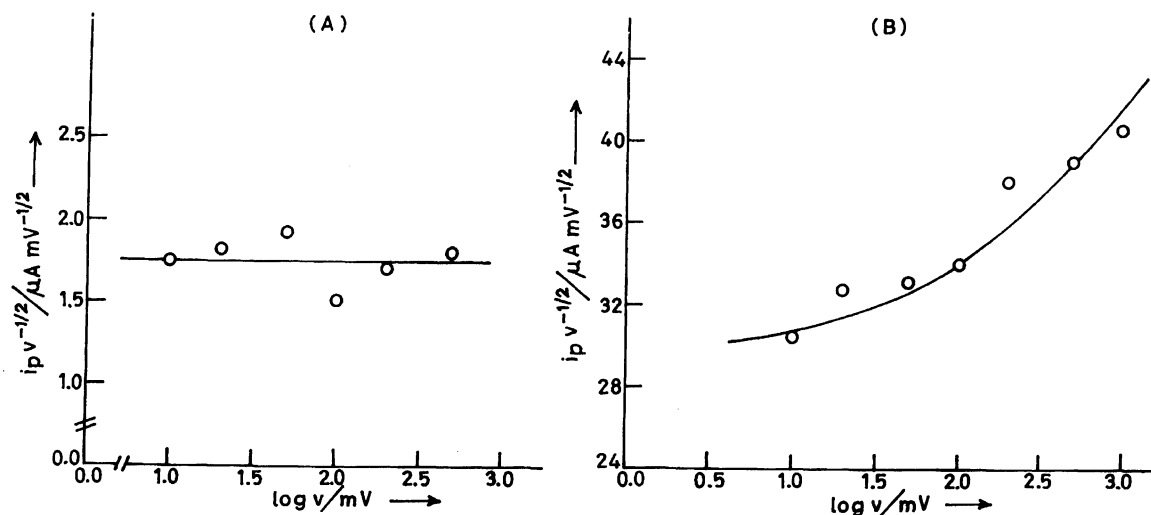


Fig. 4. Observed dependence of the peak current function ( $i_p/\sqrt{v}$ ) with variation in log v at pH 7.3. (A) Pt, (B) GCE.

$pK_a$  of 1,3,7-trimethyluric acid, and was similar to the  $pK_a$  value reported in the literature.<sup>9,10</sup> The  $pK_a$  value determined for 1,3,7-trimethyluric acid was also similar to that observed from an  $E_p$  vs. pH plot. It was thus concluded that below  $pK_a$  1,3,7-trimethyluric acid exists as a neutral species, and at pH >  $pK_a$  as a monoanion. Also, the methyl group being electron donating in nature, causes protonation of the 1, 3, and 7-nitrogen atoms. Hence, the species predominating in the bulk of the solution at pH <  $pK_a$  is a cation having three positive charges, and that at pH >  $pK_a$  is an anion with three positive charges (Chart 1).

Spectral studies during the electrooxidation of 1,3,7-tri-

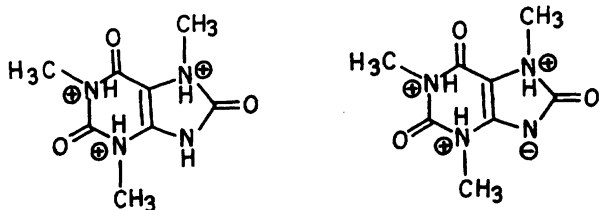


Chart 1.

methyluric acid at peak  $I_a$  potentials in the pH range 2.1–10.2 were carried out at different electrodes. At pH 5.2, a 0.1 mM solution of 1,3,7-trimethyluric acid exhibited three bands at 288, 236, and 200 nm. Upon the application of a potential 100 mV more positive than peak  $I_a$ , the absorbance at all three maxima systematically decreased (Fig. 5A curves 2 to 9). Curve 10 was recorded after 3 h of electrolysis, and exhibits a single band at 200 nm of the final product. The spectral changes observed at platinum and glassy carbon were also identical (Fig. 5 B, C) to that observed at PGE. If the same experiments were carried out, except that 15–20 min after the electrolysis potential was turned off, spectral changes similar to Fig. 5D were observed. Thus, the absorbance in the 190 and 300 nm region continued to decrease. It was therefore concluded that the intermediate species generated during electrolysis largely decayed away in a follow-up chemical reaction.

The kinetics of the decomposition of the UV-absorbing intermediate species generated upon the electrochemical oxidation of 1,3,7-trimethyluric acid was monitored at different pH and at different electrodes. For this purpose, a solution

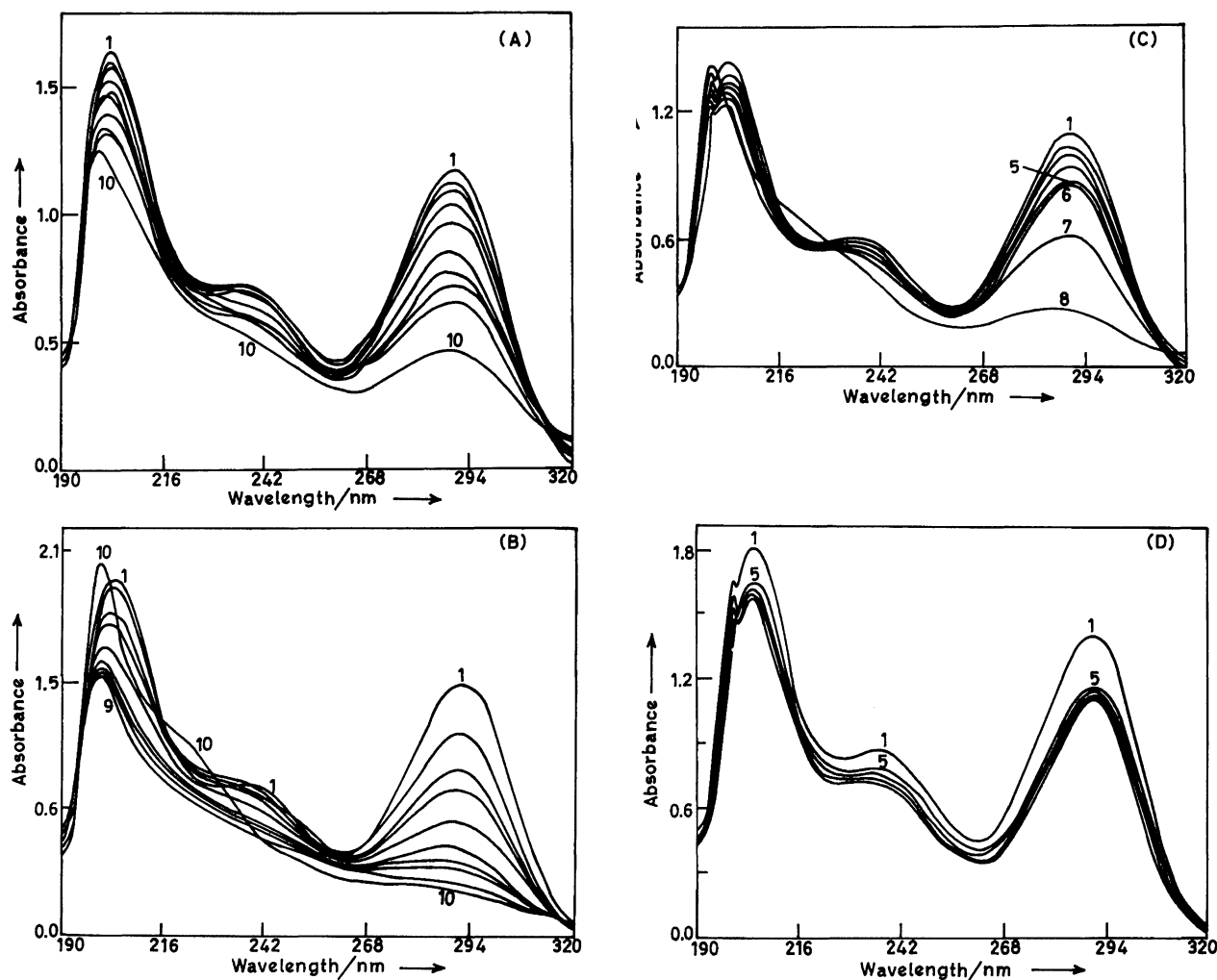


Fig. 5. Observed spectral changes during electrooxidation of 0.1 mM 1,3,7-trimethyluric acid at different solid electrodes at pH 5.2. Pot. 0.60 V vs. SCE. (A) PGE; Curves were recorded at (1) 0; (2) 5; (3) 10; (4) 20; (5) 30; (6) 45; (7) 60; (8) 80; (9) 95; (10) 180 min of electrolysis. (B) Platinum electrode; Curves were recorded at (1) 0; (2) 5; (3) 10; (4) 15; (5) 20; (6) 25; (7) 30; (8) 35; (9) 45; (10) 150 min of electrolysis. (C) GCE; Curves were recorded at (1) 0; (2) 5; (3) 10; (4) 15; (5) 25; (6) 35; (7) 160 min of electrolysis. (D) Spectral changes observed at GCE after turning off the potential corresponding to Curve 5 in Fig. 5 (C). Curves were recorded at (5) 0; (6) 5; (7) 10; (8) 17 min after switching off the potential.

of compound **I** was oxidized at the desired pH using PGE/Pt or GCE as the working electrode. When 50% of **I** was oxidized, the potential was turned off, and the absorbance at predetermined wavelengths were monitored as a function of the time. The value of  $A_{\infty}$  was established when the absorbance became constant for a sufficient period of time (8–10 min). It was interesting to observe that  $A_{\infty} \neq 0$  over the entire wavelength region monitored due to the absorption of products. At each electrode, the plots of  $\log(A - A_{\infty})$  versus time (Fig. 6) were linear, thus indicating that the decomposition of UV-absorbing intermediate follows first-order kinetics. The values of  $k$  are in the 0.002 to 0.003  $\text{s}^{-1}$  range, and are summarized in Table 4. The identical values of  $k$  at all three electrodes and at different pH further suggested that the same UV-absorbing intermediate was generated at each of the three electrodes over the entire pH range studied.

Spectral studies of the electrooxidation of 1,3,7-trimethyluric acid at peak  $I_a$  potentials, followed by reduction at peaks

Table 4. Comparison of Rate Constants Observed for 0.1 mM 1,3,7-Trimethyluric Acid at Different Electrodes at pH 5.2

Electrode	Pot. (V) vs. SCE	$k / \text{s}^{-1}$		
		288 nm	236 nm	200 nm
Platinum	0.60	0.0021	0.0021	0.0024
GCE	0.60	0.0029	0.0028	0.0022
PGE	0.60	0.0022	0.0026	0.0030
Enzymic	—	0.0026	0.0029	0.0029

$II_c$  and  $III_c$ , were also carried out at PGE in the 3.0–9.0 pH range, where peaks  $II_c$  and  $III_c$  were clearly observed. Some typical spectral changes observed at pH 7.3 are presented in Fig. 7. If the potential of the working electrode was potentiostated at  $-0.65$  V, after 45 min of oxidation (Curve 2, Fig. 7) the observed spectral changes produced Curves 3 to 8 in Fig. 7. Thus, the absorbance started increasing

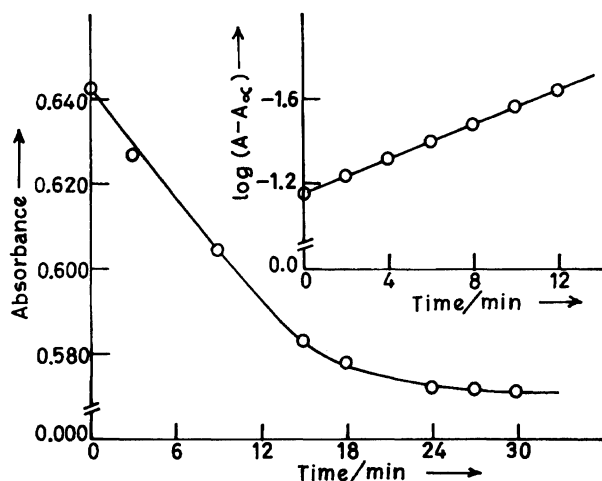


Fig. 6. Plot of absorbance vs. time and  $\log(A - A_\infty)$  vs. time for the decay of the UV-absorbing intermediate generated during electrooxidation of 1,3,7-trimethyluric acid at GCE, pH=5.2,  $\lambda=236$  nm.

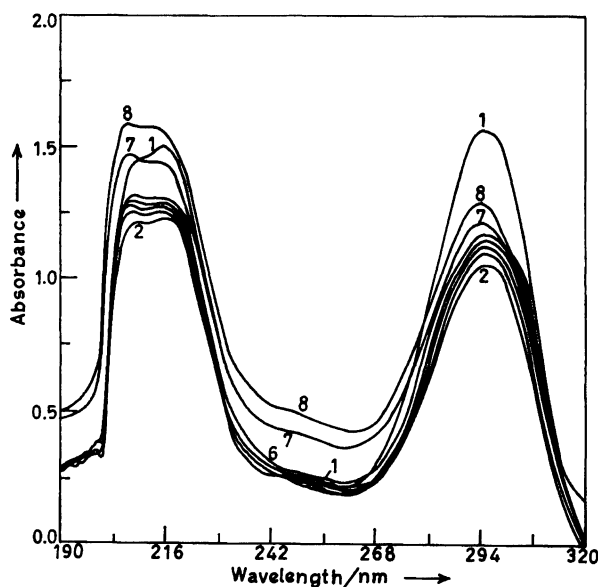


Fig. 7. Spectral changes observed for the electrooxidation followed by reduction of 0.1 mM 1,3,7-trimethyluric acid at PGE, pH=7.2. Oxidation at 0.60 V was carried out for 45 min (Curve 2) and then switched to  $-0.65$  V vs. SCE. Curves were recorded at (3) 10; (4) 20; (5) 30; (6) 40; (7) 60, and (8) 75 min.

systematically in the 200–300 nm region (Curves 3–7). Curve 8 was recorded after 77 min of electroreduction; the UV-spectrum of the formed material was identical to that of 1,3,7-trimethyluric acid. This spectral behavior revealed that the reduction of the UV-absorbing intermediate generated in the peak- $I_a$  reaction gave back the starting material.

**Product Characterization.** The products of the electrooxidation of 1,3,7-trimethyluric acid were separated and analyzed at pH 3.0 and 7.0 at all three electrodes using various analytical techniques.

The exhaustively electrolyzed solution at pH 3.0 exhibited

two spots in TLC having  $R_f$  values of 0.46 and 0.66, indicating the formation of two products during the oxidation of 1,3,7-trimethyluric acid. The liquid chromatogram exhibited three peak ( $P_1$ ,  $P_2$ , and  $P_3$ ) at pH 3.0. Peak  $P_1$ , obtained between 140–180 ml, was found to contain phosphate, and was thus discarded. The volume under the second peak ( $P_2$  180–190 ml) was collected and freeze-dried. The colorless material had a mp of  $92^\circ\text{C}$  and  $R_f=0.66$ . The mass spectrum of the material gave a molecular ion peak at  $m/z=74$ , thus suggesting the product to be *N*-methylurea. The other high-mass peaks observed in the fragmentation pattern were at 45.0 (35.4%); 44.0 (100%); 43.1 (18.8%) and 42.1 (5.6%).

The formation of *N*-methylurea as one of the products indicated that the electrooxidation of 1,3,7-trimethyluric acid caused a rupture of the imidazole ring at pH 3.0. The material obtained corresponding to peak  $P_3$  (210–250 ml) on lyophilization gave a colorless material with  $R_f=0.46$ . The mass spectrum of the material exhibited a molecular-ion peak at  $m/z=170$  (88.2%). It had a mp of  $220^\circ\text{C}$ , and exhibited major peaks in the mass spectrum at 142 (72.4%); 144.0 (58.0%); 58.1 (100%); 57.1 (78.5%), and 56.1 (81.6%). However, no attempts were made to explain the fragmentation pattern.

The  $^1\text{H}$ NMR spectrum of the material exhibited signals at  $\delta=7.78$  (s, 2H); 3.38 (s, 3H) and 3.2 (s, 3H); the product was thus characterized as 1,3-dimethylalloxan monohydrate. Upon adding  $\text{D}_2\text{O}$ , the signal at  $\delta=7.78$  disappeared, thereby confirming that it was due to the water molecule attached to 1,3-dimethylalloxan.

At pH 7.0, the exhaustively electrolyzed solution of 1,3,7-trimethyluric acid in gel permeation chromatography gave two major peaks. The first chromatographic peak (140–190 ml) was due to phosphate, and was thus discarded. The other peak (230–260 ml) on lyophilization gave a colorless material having a molar mass of  $m/z=187$ . This product is similar to the 5-hydroxyhydantoin-5-carboxamide observed in the oxidation of uric acid at PGE by Goyal et al.<sup>16)</sup> Thus, with increasing pH, the pyrimidine ring apparently becomes less stable, and, hence, ring opening, deamination and decarboxylation give 5-hydroxy-1-methylhydantoin-5-(*N*-methylcarboxamide). The formation of this product was further confirmed by its silylation using pyridine and BSA as silylating reagents. The silylated derivative exhibited a peak in a GC-Mass analysis at around 28.4 min, and exhibited a molar mass of 331 (64%). Thus, out of the three available sites only two undergo silylation. Since the  $-\text{OH}$  group present at position 5 is situated between  $>\text{C}=\text{O}$  and the  $\text{N}_4-\text{CH}_3$  group, it is expected to be silylated only at two positions due to the bulky nature of the silyl group. 5-hydroxyhydantoin-5-carboxamide has also been found to exhibit the same behavior upon silylation.<sup>17,18)</sup>

**Enzymic Oxidation.** Cyclic voltammogramic changes were monitored during the enzymic oxidation of 1,3,7-trimethyluric acid in order to detect the formation of the species responsible for peak  $II_c$ . Cyclic voltammograms at pH 5.2 at PGE were recorded with the initial sweep in the negative direction. Curve (A) in Fig. 8 represents a voltammogram of

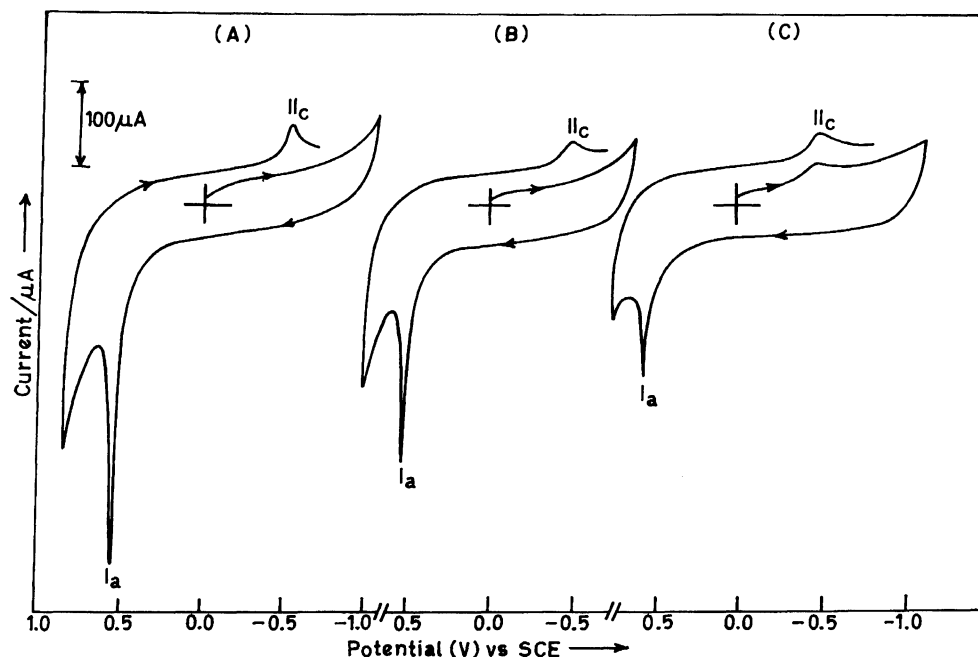


Fig. 8. Cyclic voltammograms observed during enzymic oxidation of 0.1 mM 1,3,7-trimethyluric acid in phosphate buffer of pH 5.2,  $\mu=0.25$  mM. (A) 0.1 mM 1,3,7-trimethyluric acid. (B) after adding 0.002 mM horseradish peroxidase. (C) after adding 0.6 mM  $\text{H}_2\text{O}_2$  in (B).

a 0.1 mM solution of 1,3,7-trimethyluric acid in a phosphate buffer of pH 5.2. Curve (B) represents the voltammogram after the addition of peroxidase (0.002 mM). In both curves, peak  $\text{II}_c$  was not observed in the first negative sweep. When  $\text{H}_2\text{O}_2$  (0.6 mM) was added to initiate oxidation, and cyclic voltammograms were recorded, it was observed that peak  $\text{II}_c$  started appearing during the first negative sweep at the same potential as that observed during electrochemical oxidation. It was thus inferred that a species, reducible at peak  $\text{II}_c$  potentials, is generated during enzymic oxidation, which is similar to that generated electrochemically. The spectral changes during enzymic oxidation were studied in phosphate buffers at different pH. At pH 5.2 a 0.1 mM solution of 1, 3,7-trimethyluric acid containing peroxidase exhibited two well-defined  $\lambda_{\text{max}}$  at 292 and 205 nm and a shoulder at 236 nm. Upon adding  $\text{H}_2\text{O}_2$  (0.6 mM), a systematic decrease in absorbance (as shown in Fig. 9) was observed. When the oxidation was terminated by adding the catalase, a decrease in the absorbance in the 200 to 300 nm region was observed. Thus, the spectral changes during enzymic oxidation were identical to that observed during electrochemical oxidation.

The kinetics of the decay of a UV-absorbing intermediate generated during enzymic oxidation was studied by quenching the reaction by the addition of catalase when the absorbance at 292 nm reached ca. 50%. The change in absorbance with time was monitored, and an exponential decay was noticed (Fig. 10). The value of the rate constant ( $k$ ) was determined from a plot of  $\log(A - A_\infty)$  versus time. The values of the observed rate constant were similar to that observed for electrochemical oxidation, and are presented in Table 4. Thus, the similarity in the UV spectral changes, rate constant ( $k$ ) values and appearance of peak  $\text{II}_c$  in cyclic

voltammograms indicate the possibility of a similar mechanism for the oxidation of 1,3,7-trimethyluric acid by enzyme peroxidase, and at the surface of the solid electrodes.

**Redox Mechanism.** On the basis of the obtained results it can be concluded that the oxidation of 1,3,7-trimethyluric acid occurs in a  $2e, \text{H}^+$  reaction to give methylated alloxan and *N*-methylurea at pH 3.0 and 5-hydroxy-1-methylhydantoin-5-(*N*-methylcarboxamide) at pH 7.0 as major products.

The  $E_p$ , pH dependence suggests that the conjugate base is the species oxidized over the entire pH range studied. Since

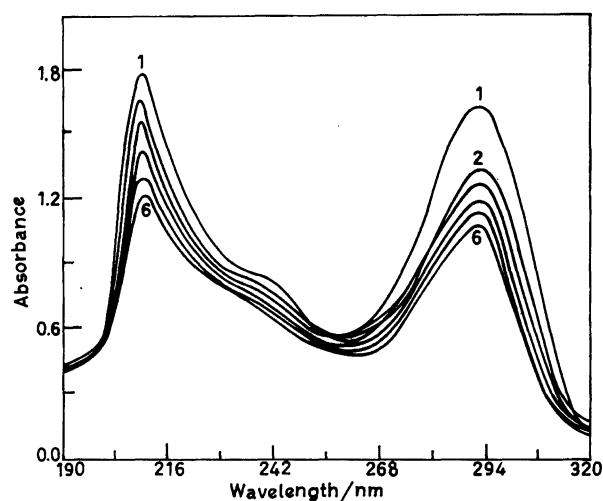


Fig. 9. Spectral changes observed during enzymic oxidation of 0.1 mM 1,3,7-trimethyluric acid, pH 5.2. Curves were recorded at (1) 0; (2) 3; (3) 6; (4) 9; (5) 13; (6) 20 min of adding  $\text{H}_2\text{O}_2$  (0.6 mM).

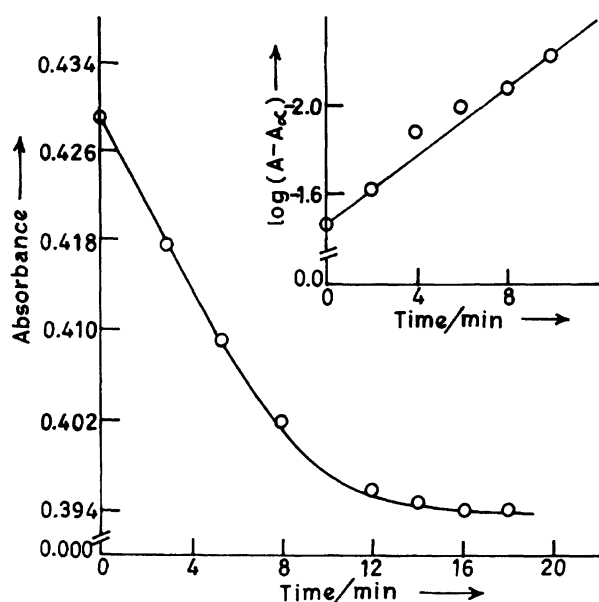
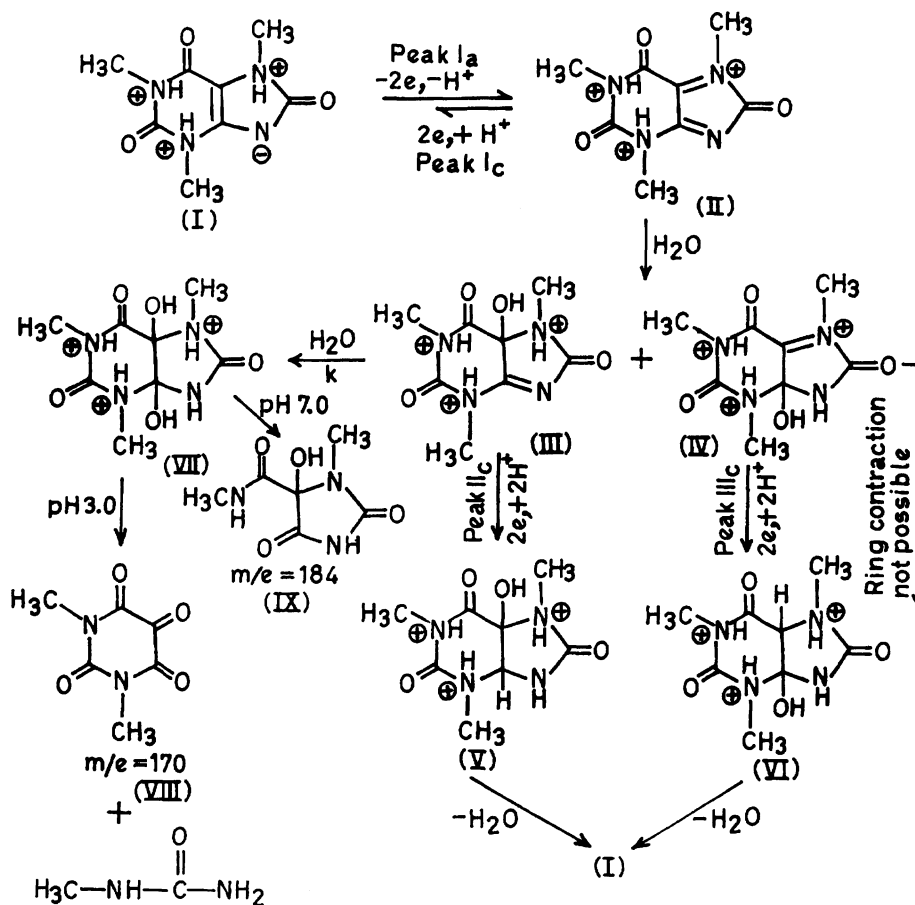


Fig. 10. The plots of absorbance versus time and  $\log(A - A_{\infty})$  versus time for the decay of the UV-absorbing intermediate generated during enzymic oxidation of 0.1 mM 1,3,7-trimethyluric acid at pH 5.2,  $\lambda = 236$  nm.

coulometric studies indicated the value of  $n$  to be  $2.0 \pm 0.3$ , it seems reasonable to conclude that 1,3,7-trimethyluric acid undergoes oxidation in a  $2e, H^+$  reaction to give diimine (II) (Scheme 1). The formed diimine seemed to be unstable as peak  $I_c$  increased along with an increase in the sweep rate. The increase in the ratio of peaks  $I_c/I_a$  with an increase in the sweep rate in the  $5 \text{ mV s}^{-1}$ — $1 \text{ V s}^{-1}$  range further supported the unstable nature of the species responsible for peak  $I_c$ . The half life of the diimine generated during the oxidation of uric acid has been reported to be 20–30 ms;<sup>19)</sup> hence, it is not unusual that species II would also be unstable in nature. An attack of water on diimine II can lead to the formation of imine alcohol III and IV. Since both imine alcohols possess positive charges in pyrimidine as well in the imidazole rings, ring contraction is not possible, and, hence, the formation of an allantoin derivative via 1-carboxy-3,7-dioxo-2,4,6,8-tetraazabicyclo-[3.3.0]oct-4-ene is not possible. The reductions of species III and IV are possible because both possess an unsaturated  $C=N$  linkage. Since the reduction of  $C=N$  in species IV involves a steric hindrance, it is most likely reducible at higher negative potentials.

Therefore, peak  $II_c$  is assigned to the reduction of species III, and peak  $III_c$  to the reduction of imine alcohol IV, which in a  $2e, 2H^+$  step gives compounds V and VI, respectively. Species V and VI formed by the reduction of imine alcohols



Scheme 1. Tentative mechanism proposed for the electrooxidation of 1,3,7-trimethyluric acid.



rapidly lose a water molecule, giving back the starting compound, 1,3,7-trimethyluric acid. It is interesting to note that peaks  $II_c$  and  $III_c$  never appeared at GCE or Pt over the entire pH range studied, thereby suggesting adsorptive activation of 1,3,7-trimethyluric acid at the surface of PGE. Adsorptive activation of organic compounds at PGE has been reported in the literature by a large number of workers.<sup>20)</sup>

The absorbance-versus-time changes observed during spectral studies (Fig. 6) represents the conversion of imine alcohols to diol (VII) by an attack of one molecule of water. Since the half life of diimine (II) is very short, the formation of imine alcohols is almost instantaneous. The loss of the N=C linkage present in (III) and (IV) during hydration causes a decrease in the absorbance, as has been observed at various electrodes. The decomposition of diol at pH 3.0 occurs in the imidazole ring, giving 1,3-dimethylalloxan and *N*-methylurea as the major products, which have been characterized by the <sup>1</sup>HNMR and mass spectrum. It is well documented in the literature that the imidazole ring of purines undergoes a rapid cleavage in an acidic medium.<sup>21,22)</sup> Hence, the formation of 1,3-dimethylalloxan and *N*-methylurea as the major products at pH 3.0 is not unusual.

In contrast to pH 3.0, where 1,3-dimethylalloxan and *N*-methylurea were observed as the major products, only 5-hydroxy-1-methylhydantoin-5-(*N*-methylcarboxamide) was obtained at pH 7.0. The formation of compound IX indicates that a cleavage of the pyrimidine ring occurs at pH 7.0, giving a hydantoin derivative as the major product. The unstable nature of the pyrimidine ring of purines under neutral and alkaline conditions has been reported for a large number of reactions.<sup>23,24)</sup>

It is concluded on the basis of these studies that the electrochemical oxidation of 1,3,7-trimethyluric acid at different solid electrodes proceeds by an identical mechanism. The identical rate constants for the decay of a UV-absorbing intermediate and the appearance of peak  $II_c$  in the first negative sweep during enzymic oxidation further indicated that the electrochemical and enzymic oxidation follow essentially a similar path.

One of the authors (NJ) is thankful to the Council of Scientific and Industrial Research, New Delhi, for the award of a Senior Research Fellowship. Financial assistance for this work was provided by the Department of Science and

Technology, New Delhi, through grant No. SP/S1/G.21/91.

## References

- 1) T. E. C. Peterson and A. B. Toth, *J. Electroanal. Chem.*, **239**, 161 (1988).
- 2) R. N. Goyal, V. Bansal, and M. S. Verma, *Bull. Soc. Chim. Fr.*, **130**, 146 (1993).
- 3) R. N. Goyal and M. S. Verma, *J. Chem. Soc., Perkin Trans. 2*, **1993**, 1241.
- 4) R. N. Goyal, A. Mittal, and D. Agarwal, *Can. J. Chem.*, **72**, 1668 (1994).
- 5) G. D. Christian and W. C. Purdy, *J. Electroanal. Chem.*, **3**, 363 (1962).
- 6) R. N. Goyal, S. K. Srivastava, and R. Agarwal, *Bull. Soc. Chim. Fr.*, **1985**, 606.
- 7) H. K. Chan and A. G. Fogg, *Anal. Chim. Acta*, **105**, 423 (1979).
- 8) J. J. Lingane, "Electroanalytical Chemistry," 2nd ed, Wiley Interscience, N. Y. (1966), p. 222.
- 9) E. A. Johnson, *Biochem. J.*, **51**, 133 (1952).
- 10) F. Bergman and S. Dikstein, *J. Am. Chem. Soc.*, **77**, 691 (1955).
- 11) R. S. Nicholson and I. Shain, *Anal. Chem.*, **39**, 706 (1964).
- 12) R. H. Wopschall and I. Shain, *Anal. Chem.*, **39**, 1514 (1967).
- 13) P. H. Reiger, "Electrochemistry," Prentice Hall, N. J. (1987), p. 343.
- 14) L. Meites, in "Physical Methods of Chemistry," ed by A. Weissberger and B. W. Rossiter, Wiley Interscience, N. Y. (1971).
- 15) G. Cauquis and V. D. Parker, "Organic Electrochemistry," ed by M. M. Baizer, Marcel Dekker, N. Y. (1973), p. 134.
- 16) R. N. Goyal, A. B. Toth, and G. Dryhurst, *J. Electroanal. Chem.*, **131**, 181 (1982).
- 17) A. C. Conway, R. N. Goyal, and G. Dryhurst, *J. Electroanal. Chem.*, **123**, 242 (1981).
- 18) R. N. Goyal and V. Bansal, *Indian J. Chem., Sect. B*, **34B**, 190 (1995).
- 19) J. L. Owens, H. H. Thomas, and G. Dryhurst, *Anal. Chim. Acta*, **96**, 89 (1978).
- 20) R. E. Vasquez, M. Hono, A. Kitani, and K. Saski, *J. Electroanal. Chem.*, **196**, 397 (1985).
- 21) A. Albert and D. J. Brown, *J. Chem. Soc.*, **1954**, 2060.
- 22) R. K. Robins, "Heterocyclic Compounds," ed by R. C. Elderfield, John Wiley and Sons, N. Y. (1967), Vol. 8, p. 162.
- 23) V. H. Brederick, F. Effenberger, and G. Rainer, *Justus Liebig Ann. Chem.*, **673**, 82 (1964).
- 24) E. Shaw, *J. Org. Chem.*, **27**, 883 (1962).